

GaN-based Semiconductor Devices for Terahertz Technology

Yue Hao, Lin-An Yang* and Jin-Cheng Zhang

Key Lab of Wide Band Gap Semiconductor Materials and Devices,

Xidian University, Xi'an, 710071, China

*Email: layang@xidian.edu.cn

Abstract: The advantages of the properties of GaN over traditional III-V materials are discussed for applications in terahertz (THz) regime. Consequently the GaN-based devices which include electronics and photonics devices are investigated with emphases on the theoretical and practical developments of Quantum Cascade Lasers, Plasma Wave FETs and Negative Differential Resistance diodes. The results demonstrate that GaN is a promising material for THz semiconductor devices with an excellent performance in operating temperature, frequency and output power. It is found that the dislocations in GaN crystal seriously impact on the performance of THz devices. It is also shown that a great progress of MOCVD technique gives the potential in GaN epitaxial growth for THz applications. Finally, our recent jobs in GaN fabrication are revealed to demonstrate the further researches in THz regime.

Keywords: Terahertz, GaN, Quantum cascade laser, Plasma wave, Negative differential resistance.

doi: 10.11906/TST.051-064.2008.06.07

I. Introduction

Terahertz (THz) regime, roughly corresponding to the frequencies from 100 GHz to 10 THz (3 mm to 30 μm), has attracted many attentions in the last decade because of its promising applications in medical, biological and industrial imaging, broadband and safety communication, radar, space science, etc. The so called "terahertz gap" implies that a big challenge still occurs for THz technology since it is in the margin of electronics and photonics technologies. There have existed two technology roadmaps for THz semiconductor devices. From low side of THz frequency, the electronics-based devices such as Gunn diode, impact avalanche transit time (IMPATT) diode, resonant tunneling diode which are based on negative differential resistance (NDR), and the nanometer field effective transistors (FET) based on plasma wave, are widely investigated for THz frequencies. From high side, the photonics-based devices such as quantum cascade laser (QCL) extend the emission wavelengths from mid- and far-infrared to THz spectral range. All the efforts are to pursue the effective radiation and detection of terahertz signals. This is due to the fact that the radiation power and the detection sensitivity of THz devices are extremely low compared with the millimeter wave devices and optoelectronic devices^[1].

GaAs-based heterostructure devices have found rapid developments in basic and applied researches for THz technology. However, the limitation of GaAs material impacts on the performance of THz devices especially in the output power and the operating temperature. In recent years, a significant progress of wide band gap semiconductor promotes GaN as a perspective candidate in THz regime. A comparison of the

figure-of-merits between GaN and GaAs materials shows that a higher critical field (2 MV/cm vs. 0.4 MV/cm) can supply higher output power density, a higher electron saturation velocity (2×10^7 cm/sec vs. 1×10^7 cm/sec) can yield ultrafast transition time therefore higher frequency, and a higher thermal conductivity (1.3 W/cmK vs. 0.5W/cmK) can suffer from higher operating temperature for GaN-based devices. Other outstanding characteristics of GaN material are unveiled in the following details.

This paper addresses GaN related devices for THz applications with emphases on QCL, Plasma Wave FETs and NDR-based diodes which are employed as THz emitters or detectors. The latest developments in GaAs THz devices are also presented in order to compare as well as discussions including most of the state of the art of researches in THz semiconductor devices.

II. GaN THz QCL

Quantum cascade laser is based on intersubband transitions in multiple quantum wells (MQWs). The first QCL employing InGaAs/InAlAs MQWs was realized in 1994^[2]. From then on, a rapid progress has been shown in its performance. Once available of the first THz QCL based on AlGaAs/GaAs in 2002^[3], it has become one of the most attractive optoelectronic devices in THz regime. Currently, the maximal output power of GaAs-based THz QCL with PW mode has approached 250 mW at 10K^[4], the wavelength has extended to 190 μm at T=64K with CW mode^[5], and the highest operating temperatures of 170K and 117K has been observed with PW and CW modes respectively^[6]. Using these lasers and a 320 \times 240 pixel focal-plane array camera, the real-time THz imaging was performed at a rate of 20 frames/sec^[7].

GaN material possesses a large electron effective mass ($m^*=0.2\sim 0.3m_0$) and a large longitude optical (LO) phonon energy ($E_{LO}\sim 90$ meV) compared with GaAs ($E_{LO}\sim 36$ meV). Moreover, the very short intersubband scattering times of ≤ 150 fs at $\sim 4.5\mu\text{m}$ wavelength and ~ 370 fs at $\sim 1.55\mu\text{m}$ wavelength have been obtained by measuring AlGaIn/GaN heterostructures quantum well at room temperature, the results at least an order of magnitude lower than that of InGaAs/GaAs quantum well^[8,9]. Thus GaN-based QCL can easily extend its emission wavelength to THz range and cover the GaAs reststrahlenband of 30~40 μm . The design and Monte Carlo simulation of THz QCL based on AlGaIn/GaN also demonstrated the excellent optical gain and

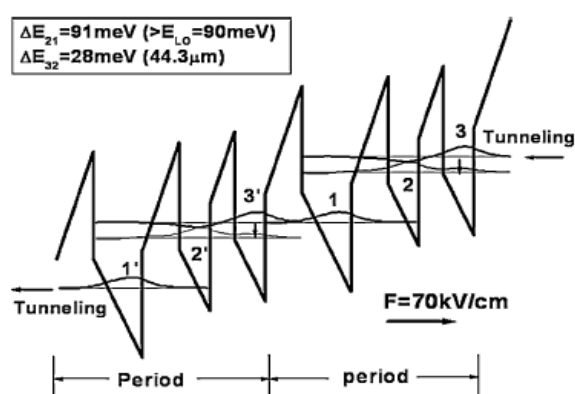


Fig. 1. Band structure, subband energy separations and envelope wavefunctions of the active region of the proposed $\text{Al}_{0.15}\text{Ga}_{0.85}\text{N}/\text{GaN}$ THz QCL.^[10]

of THz QCL based on AlGaIn/GaN also demonstrated the excellent optical gain and

operating temperature [10,11,12]. In recent years, there have developed several MQW structures for active regions of GaAs THz QCL which include the chirped superlattice structure, the resonant phonon structure and the bound-to-continuum transition structure. For GaN-based THz QCL, however, a simple three-well resonant phonon structure is commonly used for active region of AlGaN/GaN quantum well, yielding a good characteristic of operating temperature. Fig.1 gives the energy band of a typical three-well active region structure based on AlGaN/GaN for THz QCL, where three GaN wells and three AlGaN barriers have the thicknesses of 3nm/4nm/3nm/2.5nm/2nm/2.5nm from left hand of a period with an external bias of 70 kV/cm [10]. According to the theory of QCL, electrons are injected into upper laser state 3 by selective tunneling, consequently transit into lower laser state 2 after emitting photons and then rapidly depopulate to ground state 1 via resonant LO-phonon emission wherein they are transferred into the upper laser state 3' of the next period through resonant tunneling. The population inversion must be maintained during electrons transition and depopulation, inducing an effective energy band design and realization of multiple quantum wells. The energy separation between upper laser state and lower laser state is less than the LO-phonon energy ($E_{32} < E_{LO}$) in order to increase the lifetime of electrons at upper laser state by using the bottleneck effect of acoustic phonon scattering. The long relaxation times of 40~100ps have been measured in AlGaN/GaN multiple quantum wells when the intersubband transition energy is below the LO-phonon energy [13]. Meanwhile the energy separation between lower laser state and ground state is equal to or slightly larger than the LO phonon energy ($E_{21} \geq E_{LO}$) in order to approach a fast depopulation through the fast near-resonant LO-phonon emission. The characteristics of GaN material mentioned previously present many advantages over GaAs when they are employed in THz QCL: (1) a large E_{32} can be designed since a large E_{LO} therefore a longer wavelength can be realized for THz emission; (2) the design of $E_{21} \geq E_{LO}$ reduces the impact of thermal electron emission on the depopulation of electrons in lower laser state since E_{21} is far from thermal electron energy even at higher temperature, which implies that the QCL can suffer from higher temperature; (3) a large energy separation of E_{31} suppresses the probability of electrons directly transiting from upper laser state to ground state without photon emission; (4) higher in-plane kinetic energy required for phonon emission slows the electrons relaxation between 3 and 2 states thus increases the lifetime of electrons at upper laser state; (5) ultra-fast LO-phonon scattering can realize rapid depopulation of lower laser state; (6) the larger energy band discontinuity in AlGaN/GaN heterostructure increases the peak-valley ratio of NDR region, which enhances the resonant tunneling therefore accelerates the electrons relaxation of ground state.

A practical material growth of AlGaN/GaN MQW structures is shown in Fig. 2, where the 20 periods three-well active regions were manufactured by using MOCVD [14]. The TEM image in Fig. 2(a) and the XRD spectrum in Fig. 2(b) exhibit high crystalline quality of multiple layers of AlGaN/GaN. The simulation in Fig.2(b) also gives the evaluation of quantum well thickness of 3.6/4.5/3.6/2.9/2.4/2.9 nm which is very close to the design in ref.[10], demonstrating the precision of MOCVD technology. For energy band design, energy separate of $E_{32}=28$ meV corresponds to the emission wavelength of 44.3 μm ($f =$

6.67 THz), better than that of GaAs QCL in this range of frequencies. An intentional design of $E_{21}=91$ meV slightly larger than E_{LO} maintains the condition of “near-resonant LO phonon emission” in order to obtain an ultrafast depopulation. A barrier with 3 nm thickness between adjacent periods is designed to suppress the transportation of upper laser state electrons into next period, thus reducing the parasitic current.

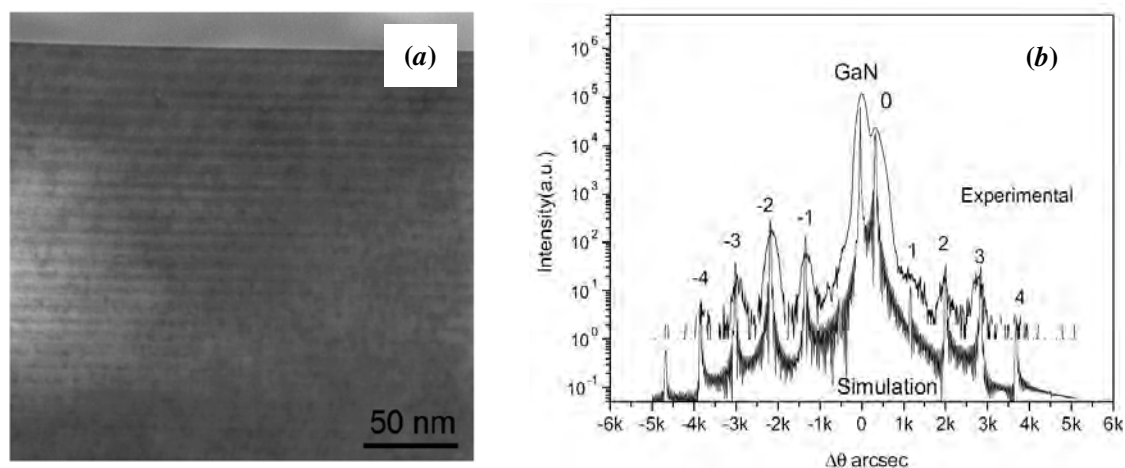


Fig. 2. AlGaIn/GaN multiple quantum wells with 20 periods, where (a) is TEM image of the sample and (b) is the measured and simulated (0002) $\omega-2\theta$ XRD spectra of the active region structure. ^[14]

The design and manufacture of waveguide for effective THz radiation of GaN QCL is also a challenge because the waveguide losses and the optical confinement have some problems due to the longer wavelength of radiation than those in mid- and far- infrared ranges. A single-surface plasmon configuration is still adopted because of its process feasible up to now ^[11]. It is predictable that some high performance waveguides such as metal-to-metal waveguide will be used in GaN THz QCL after improvement of the GaN dry-etching technology ^[15].

III. GaN Plasma Wave devices

FET based Plasma Wave devices have found rapid development in THz while semiconductor technology scaling down into the nanometer regime, where GaAs based FETs have been given much more investigations because of mature applications in microwave and millimeter wave frequencies ^[16]. In recent years, the development of GaN based heterostructure FETs has shown a great potential in plasma wave region. The concept of Plasma Wave first came from “Dyakonov-Shur Instability” in 1993 ^[17]. When the channel length of FET is shorten to sub-100 nm comparable to the mean free path of electrons, the ballistic transport dominates the electron movements between source and drain with the momentum relaxation time being longer than the electron transit time. Under the asymmetric boundary condition by external biases, for example, gate-to-source bias is short and gate-to-drain bias is open, so the originally stable electron fluid in channel becomes unstable. The coherent amplification of unstable electron fluid due to the

reflection between source and drain boundaries forms the plasma oscillation, i.e., Plasma Wave. This kind of wave in FET has a linear dispersion law with the frequency of $\omega_p = sk$, where $s = [q(U_{gs} - U_{th})/m]^{1/2}$ is the wave velocity and k is the wave vector. In ultra-short channel FETs, the wave velocity can easily approach the magnitude of 10^8 cm/sec, much larger than the electron drift velocity. This is why the frequency of plasma wave is much higher than f_T and f_{max} of the devices. Thus the FETs based on plasma wave mechanism can be used in THz regime. Importantly, the plasma oscillation in FET channel can result in a periodic variation of the channel charge and the gate mirror image charge which leads to the corresponding electromagnetic radiation in THz frequencies. Furthermore, the electromagnetic radiation can be controlled by changing the gate bias. On the other hand, the external THz radiation source can also excite the plasma oscillation in the channel. The nonlinearity of the plasma wave and asymmetric source-drain boundary conditions induce a constant voltage drop at drain terminal which can be extracted as a signal. This property is used to detect THz signal with good responsibility and sensitivity. Further, the dependence of electron density on gate bias in the channel makes the THz detector tunable [17, 18].

Original FETs for plasma wave are single gate heterostructure FETs, in which the plasma wave occurs either in the gated region or in the ungated region of channel. The gated plasmons mode is attractive because the plasmon resonant can be effectively controlled by gate bias. However, the gated plasmons in a single gate FET has weak coupling to THz radiation because (1) the plasmons are strongly screened by the metal gate, (2) they possess a vanishingly small net dipole moment due to their acoustic nature, and (3) the plasmons strongly leak into the ungated access regions^[19]. To circumvent these problems, the grating-gate FET with multiple gate structure has been developed where the periodic metal gates covering a large active area to increase the coupling of plasmons to THz radiations^[20]. Fig. 3 gives the schematic device structure of a large area grating-gate FET with 2DEG plasmons. In fact, with this kind of common 2D channel structures, the increment of ungated

regions, i.e., unscreened regions act as electric vibrator to enhance the interactions between the gated plasmons and unscreened regions. Thus it increases the coupling efficiency and excites higher order plasmon modes so that it can detect the higher THz

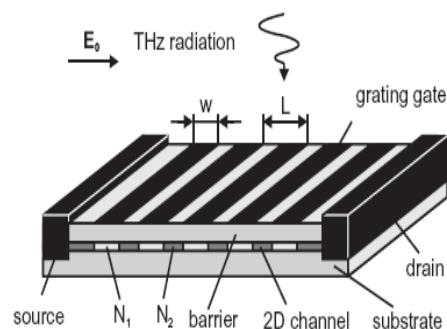


Fig. 3. Schematic of a large area grating-gate HEMT with common 2D channel.^[20]

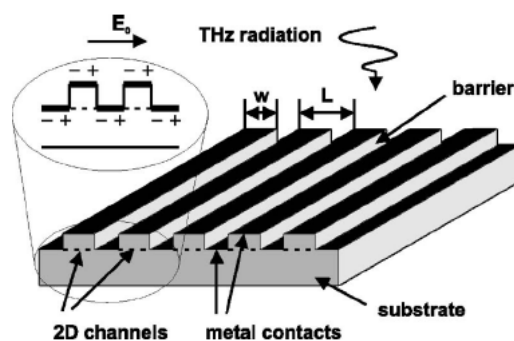


Fig. 4. Schematic of an array of HEMTs with separate 2D channel.^[19]

frequency. Meanwhile, an array of FETs with separate 2D electron channel was designed which presented an excellent high order plasmon resonance up to a frequency of 15 THz [19, 21]. The schematic FET of this kind is shown in Fig. 4 where the unscreened regions are geometrically replaced by ohmic contact. Recently, a new grating-bicoupled gate FET attracts more attentions because it enhances the plasmon excitation so as to increase the operating temperature to room temperature [22, 23]. In this device with doubly interdigitated gratings, the gates G1 and G2 present different actions. At appropriated gate biases, the gated-region under G2 continuously supplies electrons with unidirectional injection into one side of adjacent plasmon cavity under G1. This may enhance the excitation of plasmon instability, leading to room temperature operation.

GaAs based heterostructure FETs have found many applications in plasma wave devices in THz regime for the past decade. The InGaAs/InAlAs HEMT with 60 nm gate length on InP substrate was employed to yield the electromagnetic radiation of 0.4 THz ~ 1.0 THz by plasmon resonance [24]. The InGaAs/InAlAs FET with 50nm gate length has detected the THz radiation of 1.8 THz~3.1 THz at temperatures of 10 K~80 K [25]. The InGaP/InGaAs/GaAs p-HEMT with 150 nm gate length demonstrated the detections of 1.9 THz (fundamental resonance) and 5.8 THz (third-harmonic resonance) signal at room temperature [26].

Because of higher electron saturation velocity, an ultra-short transit time is obtained in GaN based FETs, especially at low temperature. This makes the bias voltage exciting the critical plasma instability below current saturation compared with the bias voltage at saturation state in GaAs FETs, which means the realization of plasmon resonance is easier in GaN FETs than in GaAs FETs [27]. The higher 2DEG density ($\sim 10^{13} \text{ cm}^{-2}$) in AlGaN/GaN heterostructure FETs gives higher plasma wave frequency, and better performance of gate modulation for resonant THz detectors. These have promoted more researches in plasma wave devices based on GaN material in THz regime. For example, a large dimension AlGaN/GaN HEMT with 1.5 μm gate length, 5 μm S/D separation and 45 μm gate width at 8K was used to yield a electromagnetic radiation of 75 GHz which much higher than f_T of 8 GHz and f_{max} of 20 GHz [27]. The AlGaN/GaN HEMT with 0.15 μm gate length produced 1.5 THz radiation at room temperature [28]. The single gate AlGaN/GaN HEMTs with the gate width of 150 μm , the gate length of 0.25 μm on sapphire and 0.15 μm on 4H-SiC substrates respectively were employed for detection of THz radiation. The noise equivalent power (NEP) method was used at the measurement temperatures of 4 K~300 K. The excellent non-resonant detection at low temperature and resonant detection at high temperature to the radiation of 0.2 THz - 2.5 THz range were observed [29]. By using the device structure in Fig. 3, a grating-gate AlGaN/GaN HEMT with a large active region area of 1.5mm \times 1.5mm was investigated [20]. The AlGaN/GaN Grating-gate HEMTs with 1 μm – 3 μm gate lengths and grating spaces of 0.5 μm and 1 μm were manufactured with epi-layer growth on sapphire substrate by MOCVD. The absorption spectra demonstrated a peak of plasmon resonance at frequency of 3 THz with 3 μm gate length and 0.5 μm grating space. Fig. 5 shows the calculated absorption spectra with the gate length of 1 μm and the grating space of 0.1, 0.3 and 0.5 μm corresponding to the curves 1, 2 and 3 [21]. It is clear that the higher order plasmon resonances can be

observed with narrow slit grating gates. The calculation shows that as high as 7th order resonance corresponding to near 10 THz radiation can be observed. With the improved schematic in Fig. 4 where the separate 2D electron channel replaces the common 2D electron channel, the excellent absorption spectra to higher order of plasmon resonances is obtained as shown in Fig. 6. The calculation shows that the curve 1 (gate length 0.8 μm , slit 0.4 μm) and curve 2 (gate length 0.5 μm , slit 0.7 μm) with separate 2D electron channel demonstrate better high order resonances absorption than curve 3 (gate length 0.8 μm , slit 0.4 μm) with common 2D electron channel [19, 21].

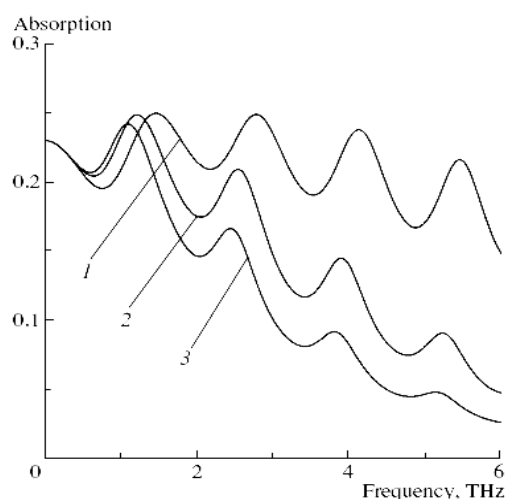


Fig. 5. Calculated absorption spectra of Grating-gate AlGaIn/GaN HEMT with common 2D electron channel. [21]

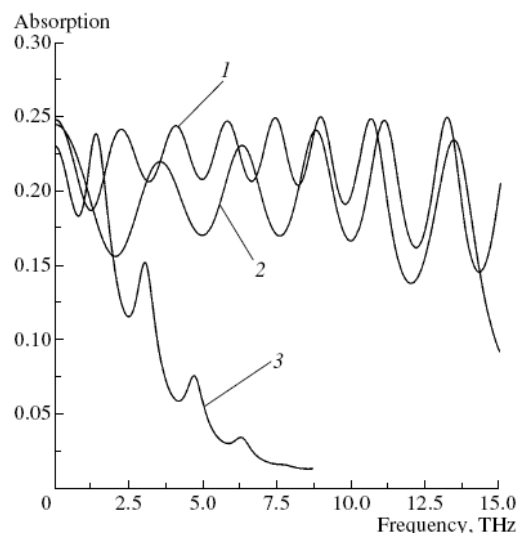


Fig. 6. Calculated absorption spectra of Grating-gate AlGaIn/GaN HEMT with separate 2D electron channel. [21]

IV. GaN NDR diodes

NDR based diodes have been applied in high frequency regime for many years. Not only the output power but also the manufacturing feasibility promotes their applications in THz regime [30]. It is well known that the advantages of GaN over GaAs and InP in higher power capability and higher operation frequency are directly related to its larger intervalley energy gap and higher peak and saturation velocities. Monte Carlo simulations demonstrated a higher NDR relaxation frequency of $f_{\text{NDR}}=740\text{GHz}$ in GaN compared with 109GHz in GaAs [31]. According to the studies of GaN band structure, the Γ -valley inflection point, at which the group electron velocity is maximal, was found to be located below the lowest satellite valley in both zinc-blende and Wurtzite GaN. The results indicated that NDR was primarily caused by the dispersion of the electron drift velocity in the Γ -valley. The inflection-based NDR presented a threshold field of 80 kV/cm and peak velocity of $3.8\times 10^7\text{cm/sec}$ compared with those of 110 kV/cm and $2.7\times 10^7\text{cm/sec}$ for intervalley-transfer-based NDR [32, 33]. This gives a very fast transit time of electrons consequently a possible capability of significantly increased frequency for GaN inflection-based NDR diodes.

The above mechanism of GaN has been widely applied for Gunn diode theoretically and practically in THz frequencies [34, 35]. The schematic and device fabrication of GaN Gunn diode are shown in Fig. 7. The Gunn diode layers were grown by MOCVD with the active layer doping varied from $1 \times 10^{17} \text{ cm}^{-3}$ to $5 \times 10^{17} \text{ cm}^{-3}$ while the thickness was $2.5 \mu\text{m}$ to $3.0 \mu\text{m}$ and the diameter was $50 \mu\text{m}$. The structure optimization of active layer thickness reducing from $3 \mu\text{m}$ to $0.3 \mu\text{m}$, doping increasing from 10^{17} cm^{-3} to 10^{18} cm^{-3} and the size shrinking from $50 \mu\text{m}$ to $10 \mu\text{m}$ was predicted to show the fundamental frequency exceeding 700 GHz [36]. To date, the challenges to the fabrication of GaN Gunn diode are still the control of threading dislocation combined with ionized impurity scattering in material growth, the formation of excellent ohmic contact and the effective etching

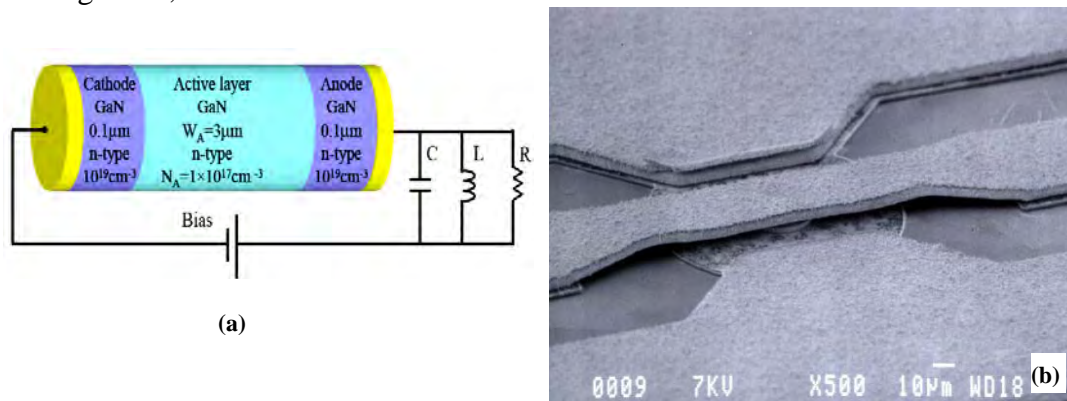


Fig. 7. Schematic of GaN NDR diode oscillator (a), and SEM photograph of fabricated device (b). [36]

techniques because of the properties of GaN material.

Resonant Tunneling Diode (RTD) is a kind of NDR based quantum device. The very high operating frequency of 420 GHz in GaAs/AlAs RTD and the frequency of 712 GHz in AlAs/AlSb RTD demonstrated their potential in THz regime. However, the output power of the order of few microwatts is a limitation for their applications. Recently, GaN based double-barrier RTD has shown excellent room temperature operation. The double-barrier quantum wells with the thickness of $2 \text{ nm}/1 \text{ nm}/0.75 \text{ nm}/1 \text{ nm}/2 \text{ nm}$ was manufactured and simulated, showing a NDR region with very high peak-to-valley current ratio of 32 and the peak current density of 180 A/cm^2 [37, 38]. The instability caused by traps was revealed [39]. This indicates that the crystalline quality of AlN/GaN multiple-epitaxial is a key issue to promote the performance of GaN RTD.

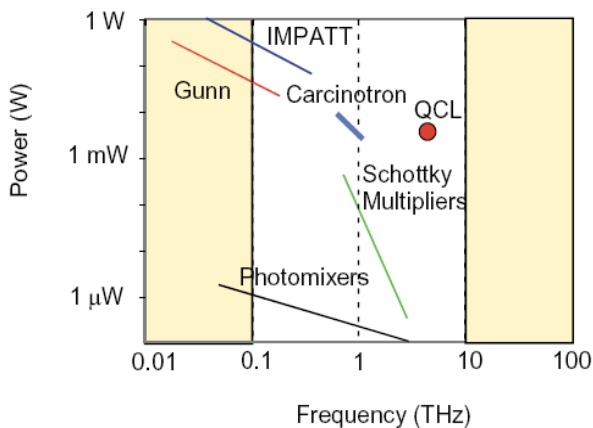


Fig. 8. Output power predictions of different devices in THz frequencies.

Traditional IMPATT diodes based on Si, GaAs and InP have shown the maximal output power compared with other diodes. The output powers of several tens of mW and several

hundreds of μW are easily obtained at 200 GHz and 400 GHz [30]. In THz frequency range, IMPATT diode also maintains its excellent output power performance. The predictions of output power of different devices are given in Fig. 8. This attracts many investigations of GaN-based IMPATT diode for high power THz radiation source because the output power of IMPATT diode is proportional to E_c^2 and v_s^2 while GaN can supply higher critical electric field E_c and electron saturation velocity v_s . An output power of 2.5W and efficiency of 17% ~ 20% was predicted at 1.45THz recently. The new structure of active region of IMPATT diode may be an effective technique to improve the frequency and output power [40, 41]. However, the device manufacturing is still immature by far due to the impact of GaN crystalline quality on the performances of high frequency and high power.

V. Growth of GaN material for THz applications

The crystalline quality of GaN is of great importance for application in THz frequencies. Many key material characteristics for THz devices such as the intersubband transition, the Γ -valley inflection and the ballistic transport, etc., are largely influenced by the defects in the bulk GaN and the heterostructure interface. Moreover, the precise control of ultra-thin multiple epi-layers are very important for MQW formation and resonant tunneling enhancement. Although molecular beam epitaxy (MBE) has been widely used in material growth, metalorganic chemical vapor deposition (MOCVD) should exhibit advantages over MBE including higher growth rates, feasible reactor design and maintenance and mass production for practical purpose. Thus the THz material fabrications by using MOCVD have shown more increase in recent literatures. Based on the independently innovated MOCVD system (XD MOCVD-320), many practical GaN heterostructures, such as AlGaIn/GaN, InGaIn/GaN, AlIn/GaN have been grown for LED and HEMT fabrications in our work. The MQWs with 5 ~ 10 periods and the superlattices with 20 ~ 60 periods were grown. The minimal growth thickness has well been controlled in the range of 1~2 nm with smooth morphologies, indicating that the devices with ultrathin barriers and wells can be realized to operate in the THz frequencies. Shown in Fig. 9(a) is the uniformity pattern of AlGaIn/GaN epitaxy on whole the 4H-SiC wafer with high temperature AlN as nucleation layer, exhibiting the practicability of the GaN epitaxial growth with RSD of ~1.42 %. While in Fig. 9(b) gives the measured electron mobilities and 2DEG densities at different temperatures, showing the mobilities of 1531 cm^2/Vs and 5207 cm^2/Vs , the 2DEG densities of $1.81 \times 10^{13} \text{ cm}^{-2}$ and $1.78 \times 10^{13} \text{ cm}^{-2}$ at 300K and 77K respectively. The dislocation densities of $\sim 10^7 \text{ cm}^{-2}$ and $1\sim 3 \times 10^8 \text{ cm}^{-2}$ are obtained respectively on GaN/4H-SiC templates with or without ELO growth technique. To evaluate the crystalline quality of GaN epi-layer, the HRXRD patterns of two samples with the structure of AlGaIn/GaN/AlN-NL/Sapphire are given in Fig. 10, where (a) is the GaN (0002) rocking curve measured by using Bruker D8 Discover XRD (sample No. XD1261), and (b) is the (0002) ω -2 θ curve measured by using Bede D1 double-crystal XRD (sample No. XDB031C). The peaks at $\omega = 0, 1002$ and 2640 arcsec correspond to GaN (0002), AlGaIn (0002) and AlN nucleation layer respectively. These results show excellent epitaxial growth of multiple-layer GaN heterostructures by employing the

home-made MOCVD system. For application in optoelectronic devices, the $\text{Al}_x\text{Ga}_{1-x}\text{N}/\text{GaN}$ material with high Al fraction ($x = 0.85$) and the pure AlN material with FWHM of 108 arcsec have also been fabricated. It is predictable that the epitaxial growth technology and the crystalline quality of GaN-based materials will show significant prospect in THz regime.

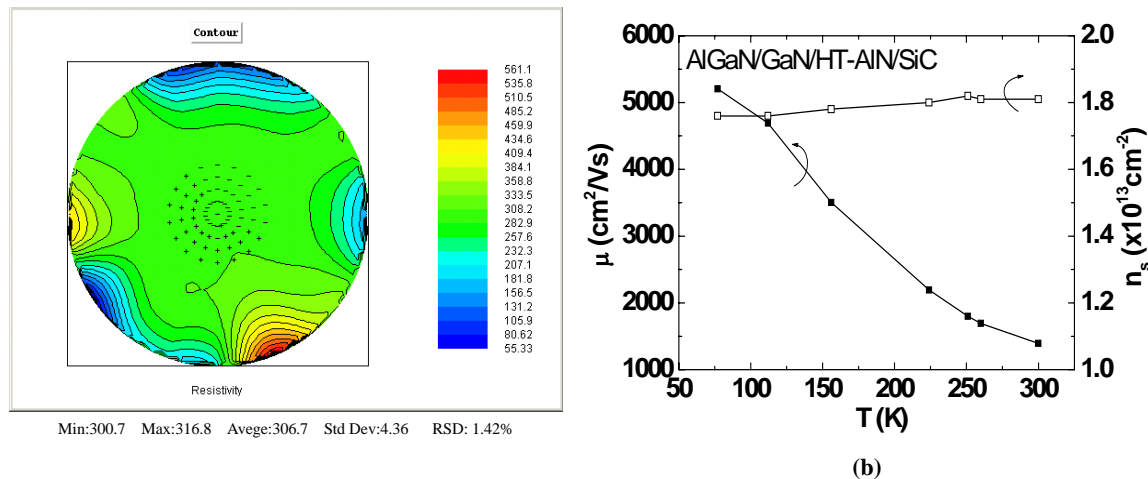


Fig. 9 Contour of the epi-layer uniformity (a), electron mobility and density (b) of AlGaIn/GaN heterostructure on 4H-SiC substrate fabricated by XD MOCVD-320 system.

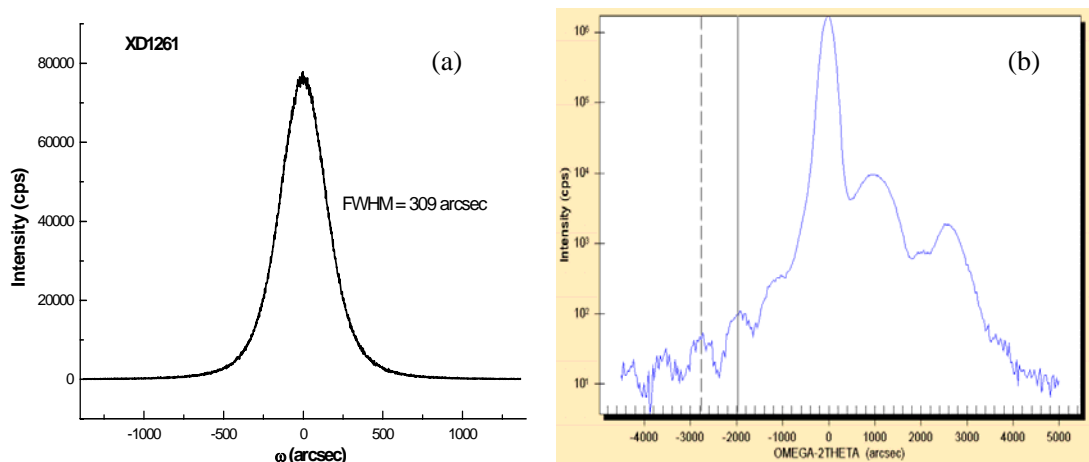


Fig. 10. XRD Measurements of $\text{AlGaIn}/\text{GaN}/\text{AlN-NL}/\text{Sapphire}$ structure, (a) is GaN (0002) rocking curve of the sample No. XD1261 and (b) is (0002) ω - 2θ curve of the sample No. XDB031C.

VI. Conclusions

The characteristic advantages of GaN over traditional III-V materials, such as GaAs, are discussed for applications in THz regime. Besides the GaN-based devices including electronics as well as photonics are investigated with emphases on the theoretical and practical developments of QCLs, Plasma Wave FETs and NDR diodes. The results demonstrate that GaN is a promising candidate for THz semiconductor devices especially in operating temperature and output power, though both of them still bottleneck the

performance of THz devices. The researches have indicated that the defect in GaN crystal has a serious impact on the performance of GaN THz devices. Furthermore, it also indicates that MOCVD technique instead of MBE has found a great progress in material growth of GaN for THz applications. Finally, our recent jobs in GaN fabrication are revealed to demonstrate the ability of the further researches in THz regime.

Acknowledgements

This work is supported by NSFC under grant No. 60676048 and grant No. 60736033.

References

- [1] M. Shur, Terahertz technology: devices and applications, *Proceedings of ESSDERC*, Grenoble, France, (2005).
- [2] J. Faist, F. Capasso, D. L. Sivco, et al., *Quantum cascade lasers*, 264, 553, (1994).
- [3] R. Kohler, A. Tredicucci, F. Beltram, et al., Terahertz semiconductor heterostructure laser, *Nature*, 417, 156~159, (2002).
- [4] B.S. Williams, S. Kumar, Q. Hu and J.L. Reno, High-power terahertz quantum cascade lasers, *Electronics letters*, 42(2), 89~90, (2006).
- [5] S. Kumar, B.S. Williams, and Q.Hu, et al., 1.9 THz quantum-cascade lasers with one-well injector, *Appl. Phys. Lett.*, 88, 121123 (2006).
- [6] B.S. Williams, S. Kumar, Q. Hu, and J.L. Reno, Operation of terahertz quantum-cascade laser at 164K in pulsed mode and at 117K in continuous-wave mode, *Optics Express*, 13, 331~339, (2005).
- [7] A. W. M. Lee and Q. Hu, Real-Time, Continuous-Wave Terahertz Imaging using a Microbolometer Focal-Plane Array, *Opt. Lett.*, 30, 2563, (2005).
- [8] N. Iizuka, K. Kaneko, N. Suzuki, et al., Ultrafast intersubband relaxation (<150 fs) in AlGaIn/GaN multiple quantum wells, *Appl. Phys. Lett.*, 77(8), 648~650, (2000).
- [9] J. D. Heber, C. Gmachl, H. M. Ng, and A. Y. Cho, Comparative study of ultrafast intersubband electron scattering times at ~1.55 μ m wavelength in GaN/AlGaIn heterostructures, *Appl. Phys. Lett.*, 81(7), 1237~1239, (2002).
- [10] G Sun, R. A. Soref, J. B. Khurgin, Active region design of a terahertz GaN/Al_{0.15}Ga_{0.85}N quantum cascade laser, *Superlattices and Microstructures*, 37, 107~113, (2005).

- [11] V. D. Jovanovic, D. Indjin, Z. Ikonic, et al., Simulation and design of GaN/AlGa_N far-infrared (~ 34 mm) quantum-cascade laser, *Appl. Phys. Lett.*, 84(16), 2995~2997, (2004).
- [12] N. Vukmirovic, V. D. Jovanovic, D. Indjin, Optically pumped terahertz laser based on intersubband transitions in a GaN/AlGa_N double quantum well, *J. Appl. Phys.*, 97, 103106, (2005).
- [13] E. Monroy, F. Guillot, B. Gayral, et al., Observation of hot luminescence and slow inter-sub-band relaxation in Si-doped GaN/Al_xGa_{1-x}N ($x=0.11, 0.25$) multi-quantum well structures, *J. Appl. Phys.*, 99, 093513, (2006).
- [14] G.S. Huang, T.C. Lua, H.H. Yao, et al., GaN/AlGa_N active regions for terahertz quantum cascade lasers grown by low-pressure metal organic vapor deposition, *Journal of Crystal Growth*, 298, 687~690, (2007).
- [15] Hiroaki Yasuda, Iwao Hosako, and Norihiko Sekine, Terahertz Waveguide Design for GaSb Quantum Cascade Laser, *Proceedings of Asia-Pacific Microwave Conference* (2006).
- [16] J. Łusakowski, Nanometer transistors for emission and detection of THz radiation, *Thin Solid Films*, 515, 4327~4332, (2007).
- [17] M. Dyakonov, M. Shur, Shallow Water Analogy for a Ballistic Field Effect Transistor: New Mechanism of Plasma Wave Generation by dc Current, *Physics Review Lett.*, 71(15), 2465~2468, (1993).
- [18] M. Dyakonov, M. Shur, Detection, Mixing, and Frequency Multiplication of Terahertz Radiation by Two-Dimensional Electronic Fluid, *IEEE Trans. ED*, 43(3), 380~387, (1996).
- [19] V. V. Popov, G. M. Tsymbalov, and D. V. Fateev, et al., Cooperative absorption of terahertz radiation by plasmon modes in an array of field-effect transistors with two-dimensional electron channel, *Appl. Phys. Lett.*, 89, 123504, (2006).
- [20] N. Pala, D. Veksler, A. Muravjov, et al., Resonant Detection and Modulation of Terahertz Radiation by 2DEG Plasmons in GaN Grating-Gate Structures, *IEEE SENSORS Conference*, 570~572, (2007).
- [21] V. V. Popov, G. M. Tsymbalov, T. V. Teperik, et al., Terahertz Excitation of the Higher-Order Plasmon Modes in Field-Effect Transistor Arrays with Common and Separate Two-Dimensional Electron Channels, *Bulletin of the Russian Academy of Sciences: Physics*, 71(1), 89~92, (2007).
- [22] Y. M. Meziani, T. Otsuji, M. Hanabe, Room temperature generation of terahertz radiation from a grating-bicoupled plasmon-resonant emitter: Size effect, *Appl. Phys. Lett.*, 90, 061105, (2007).
- [23] T. Otsuji, Y. M. Meziani, M. Hanabe, Emission of terahertz radiation from InGaP/InGaAs/GaAs grating-bicoupled plasmon-resonant emitter, *Solid-State Electronics*, 51, 1319~1327, (2007).
- [24] W. Knap, J. Łusakowski, T. Parenty, et al., Terahertz emission by plasma waves in 60 nm gate high electron mobility transistors, *Appl. Phys. Lett.*, 84(13), 2331~2333, (2004).

- [25] A. El Fatimy, F. Teppe, N. Dyakonova, et al., Resonant and voltage-tunable terahertz detection in InGaAs/InP nanometer transistors, *Appl. Phys. Lett.*, 89, 131926, (2006).
- [26] T. Otsuji, M. Hanabe, and O. Ogawara, Terahertz plasma wave resonance of two-dimensional electrons in InGaP/InGaAs/GaAs high-electron-mobility transistors, *Appl. Phys. Lett.*, 85(11), 2119~2121, (2004).
- [27] Y. Deng, R. Kersting, J.Z. Xu, et al., Millimeter wave emission from GaN high electron mobility transistor, *Appl. Phys. Lett.*, 84(1), 70~72, (2004).
- [28] N. Dyakonova, A. El Fatimy, J. Łusakowski, et al., Room-temperature terahertz emission from nanometer field-effect transistors, *Appl. Phys. Lett.*, 88, 141906, (2006).
- [29] A. El Fatimy, S. B. Tombet, F. Teppe, et al., Terahertz detection by GaN/AlGaIn transistors, *Electronics Letters*, 42(23), 1342~1343, (2006).
- [30] R. J. Trew, High-Frequency Solid-State Electronic Devices, *IEEE Trans. ED*, 52(5), 638~649, (2005).
- [31] B.E. Foutz, et al., Comparison of high field electron transport in GaN and GaAs, *Appl. Phys. Lett.*, 70 (21), 2849~2852, (1997).
- [32] J. Kolnik et al., Electronic Transport Studies of bulk zinc-blende and wurtzite phases of GaN based on an ensemble Monte Carlo calculation including a full zone bandstructure, *J. Appl. Phys.*, 78 (2), 1033~1038, (1995).
- [33] S. Krishnamurthy et al, Bandstructure effect on high-field transport in GaN and GaAlN, *Appl. Phys. Lett.*, 71 (14), 1999~2000, (1997).
- [34] J. T. Lu and J. C. Cao, Terahertz generation and chaotic dynamics in GaN NDR diode, *Semicond. Sci. Technol.*, 19, 451~456, (2004).
- [35] C. Sevik, C. Bulutay, Simulation of Millimeter-Wave Gunn Oscillations in Gallium Nitride, *Turk J. Phys.*, 28, 369~377, (2004).
- [36] E. Alekseev, D. Pavlidis, GaN Gunn diodes for THz signal generation, *IEEE MTT-S International Microwave Symposium Digest*, 3, 1905~1908, (2000).
- [37] A. Kikuchi, R. Bannai, and K. Kishino, et al., AlN/GaN double-barrier resonant tunneling diodes grown by rf-plasma-assisted molecular-beam epitaxy, *Appl. Phys. Lett.*, 81 (9), 1729~1731, (2002).
- [38] A. M. Kurakin, S. A. Vitusevich, S. V. Danylyuk, et al., Capacitance characterization of AlN/GaN double-barrier resonant tunnelling diodes, *Phys. Stat. Sol. (c)*, 3, No. 6, 2265~2269, (2006).
- [39] M. V. Petrychuk, A. E. Belyaev, A. M. Kurakin, et al., Mechanisms of current formation in resonant tunneling AlN/GaN heterostructures, *Appl. Phys. Lett.*, 91, 222112, (2006).
- [40] A. Reklaitis, L. Reggiani, Monte Carlo study of hot-carrier transport in bulk wurtzite GaN and

modeling of a near-terahertz impact avalanche transit time diode, *J. Appl. Phys.*, 95 (12), 7925~7935, (2004).

[41] M. Mukherjee, N. Mazumder, S. K. Roy, GaN IMPATT diode: a photo-sensitive high power terahertz source, *Semicond. Sci. Technol.*, 22, 1258~1267, (2007).